

CHAPTER 123

Suspended Sediment Concentration in the Surf Zone

Makoto Ifuku¹⁾ and Tadao Kakinuma²⁾

Abstract

The water particle velocity, the pressure fluctuation and suspended sediment concentration near the bottom were measured in the surf zone. Data were obtained on the mean sediment concentration, phase lag between onshore velocity and suspended sediment concentration. The near-bottom velocity distributions under finite amplitude waves were calculated on the basis of the turbulent boundary layer theory by using time-independent/dependent eddy viscosities and Prandtl mixing length theory. The concentrations at reference level were estimated from the Kalkanis' theory using the velocity value at the top of a sand particle and the distributions of suspended sediment concentration were calculated on the basis of the turbulent diffusion theory by using time-independent/dependent diffusion coefficients. The computed mean values of the suspended sediment concentration agree with those observed by Noda, the authors and Nielsen and those measured by Deigaard et al.. The computed phase lag agrees well with observed by the authors.

1. Introduction

In order to investigate the sediment transport phenomena in the surf zone, it is necessary to study the sediment suspension mechanism due to waves. Many investigators have been concerned with sediment suspension. Early studies, such as those of Fairchild(1959), Homma and Horikawa(1962) and Noda(1967) were made with siphons, pumped sampler and suspended sampler. With these types of sampler it is difficult to obtain accurate records of concentration variation. For these most recent studies, such as those of Homma et al.(1965), Sleath(1982), Brenninkmeyer(1974) and Wright et al.(1982) the records of concentration variation were obtained in laboratory and on site. Sleath(1982) measured the variation of sediment concentration at a fixed point above

1) Associate Professor, Department of Ocean Engineering, Ehime University, Matsuyama, Japan

2) Professor, Department of Ocean Engineering, Ehime University, Matsuyama, Japan

a ripple crest in oscillatory flow. He showed that stronger peaks in the concentration records are observed at phases where the velocity at the upper edge of the boundary layer reverses, while weaker peaks are found at phases where the velocity is approximately maximum. He expressed the characteristics of the boundary layer in oscillatory flow in terms of the vortex near the ripple and elucidated the mechanism of sediment suspension. However, in the discussion of initial motion of sediment, accurate knowledge of the near-bottom water particle velocity in the turbulent boundary layer is important in order to evaluate drag, lift, inertia and body forces acting on sediment.

The present paper deals with the details of near-bottom water particle velocity and suspended sediment concentration on the basis of field data. Meanwhile, numerical analysis has also been performed on the basis of the turbulent boundary layer theory and diffusion theory to elucidate theoretically the observed and experimental suspended sediment concentrations.

2. Field observation and data analysis

2.1 Sites and method of observations

The field observations were conducted at Baishinji coast near Matsuyama city in Ehime Prefecture, Japan, over the periods from 15 December 1982 to 19 March 1983 and from 21 December 1983 to 19 March 1984. The observation points were located 120 and 100 m off the coastal breakwater and the mean water depths at these points were 2.0 and 1.7 m (Fig. 1). The mean beach slope around both the points were approximately 0.01.

The field instrumentation system used was composed of 3 sets of two-component electromagnetic flow meters MODEL551(MARSH McBIRNEY), a pressure transducer MODEL 205-2 (Setra Systems) and a turbidimeter MODEL MA-101 RD(Hokuto Riken).

Station I

The instruments were mounted on a frame and fixed on the bottom using 8 concrete blocks.

The levels of electromagnetic flow meter were 0.07, 0.65 and 0.98 m above the bottom and the horizontal velocities were measured. The levels of the turbidimeter and the pressure transducer were 0.04 and 0.72 m above the bottom respectively.

Station II

An electromagnetic flow meter was set at the level of 0.3 m above the bottom and the cross-shore and vertical components of water particle velocity were measured. The other two were set at the levels of 0.45 and 0.70 m to measure the cross-shore and longshore components. The levels of the turbidimeter and the pressure transducer were 0.34 and 0.49 m

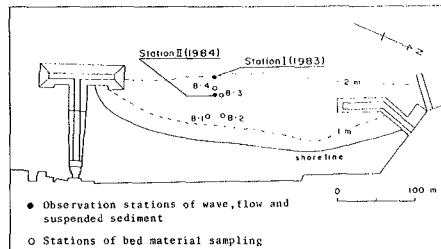


Fig.1 Observation stations of wave, flow, suspended sediment and bed material.

above the bottom respectively.

The turbidimeter was an optical type and composed of six light sources and a receiver. Data obtained were transmitted to a shore station, where they were recorded on a data logger XR-30(TEAC).

2.2 Data analyses

Records of velocity, pressure fluctuation and turbidity (suspended sediment concentration) were digitized for a interval of 0.2 s at every 15 min. The zero-up-crossing method was employed to calculate the velocity and pressure fluctuation of the significant wave. First, spectral analyses were performed to obtain the power spectrum, cross spectrum, physical spectrum of velocity and suspended sediment concentration as well as directional spectrum.

2.3 Significant wave and bed material

During the 1983 observation the significant wave height and period were 0.41-0.53 m and 4.4-4.7 s, while in 1984 they were 0.33-0.79 m and 4.4-5.3 s. The frequency of breaker occurrence is defined as the ratio of the number of breakers to the number of waves in each data set. In both years, most of breakers visually were of the spilling type. Sampling of bed material performed in November 1983 at B-1 and 2 and in January 1984 at B-3 and 4. Bed material around the observed sites consisted entirely of sand with a median diameter of 0.18 mm.

3. Results of data analysis

3.1 Power spectrum of suspended sediment concentration

The great majority of power is in the low frequency range (0.016 Hz - 0.025 Hz), although a weaker peak appears at the peak frequency of wind waves (approximately 0.25 Hz). The power of suspended sediment concentration falls off as: $f^{-0.5}$ - f^{-1} (f : frequency) and f^{-3} - $f^{-3.5}$ in the low and high frequency ranges, regardless of the frequency of breaker occurrence, while the profiles of cross-shore velocity and pressure fluctuation depend on the frequency of breaker occurrence. Fig. 2 shows the power spectrum of the suspended sediment concentration and cross-shore velocity; (a) and (b) are in the case of the low and high frequency of breaker occurrence respectively.

3.2 Suspended sediment concentration and near-bottom cross-shore velocity

Fig.3 shows the physical spectrum of cross-shore velocity observed 0.07 m above the bottom together with the time series of suspended sediment concentration observed at 0.04 m above the bottom. The uppermost figure is for the lower frequency band, 0.02-0.078 Hz; next is for 0.098-0.156 Hz; third is for the peak frequency band of wind waves, 0.176-0.234 Hz and the fourth is for 0.391-0.449 Hz. The lowest figure shows the time series of suspended sediment concentration. Energy density of the physical spectrum in the lower frequency band is approximately one-fifth as large as that in the peak frequency band. The

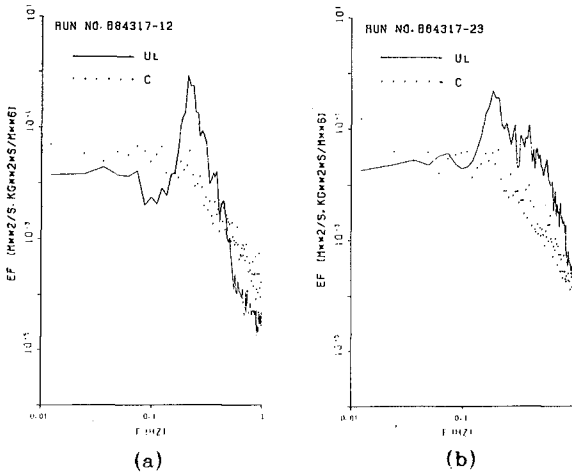


Fig.2 Power spectra of suspended sediment concentration and cross-shore velocity, where the frequencies of breaker occurrence are (a) 14 % and (b) 20 %.

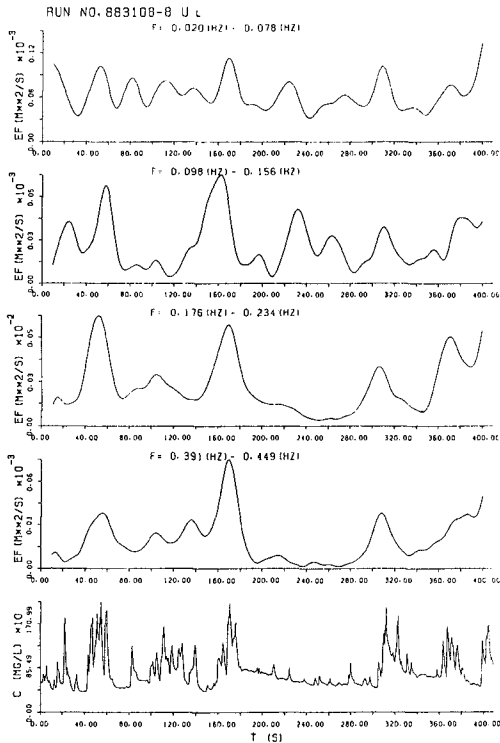


Fig.3 Physical spectra of cross-shore velocity at the level of 0.07 m and time series of suspended sediment concentration at 0.04 m above the bottom.

suspended sediment concentration is quite high when energy densities in the peak and quarter frequency bands of wind waves are high. Thus the fact that higher values of suspended sediment concentration occur at a 40-60 s time interval seems to be related to lower and peak frequency components of cross-shore velocity. The above discussion is very interesting in comparison with the results of Brenninkmeyer(1974) and Wright et al.(1982), who suggested that suspended sediment concentration is related to swells or long period waves and surf beat on the basis of power spectrum analyses of wave, cross-shore velocity and suspended sediment concentration observed in the surf zone.

3.3 Phase lag between cross-shore velocity and suspended sediment concentration

Fig.4 shows the histogram of phase lag between a peak of cross-shore velocity and that of suspended sediment concentration during a wave cycle. The histograms were obtained through the analyses of 107 and 120 waves in (a) and (b) where the frequencies of breaker occurrence are 13 % and 19 % respectively. The maximum values in the histogram appear at the phases $\pi/2$, 1.3π in (a) and $\pi/2$, 1.1π in (b).

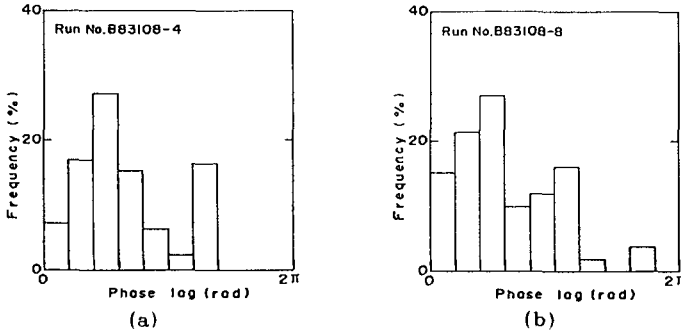


Fig.4 Histograms of phase lag between onshore velocity and suspended sediment concentration, where the frequencies of breaker occurrence are (a) 13 % and (b) 19 %.

4. Numerical analysis

4.1 Basic equations

(a) Water particle velocity in the turbulent boundary layer

The x - axis is taken along a horizontal bottom and z - axis vertically upwards. The velocity components in the x - and z - directions are denoted by u and w .

The equation of motion for a two-dimensional turbulent boundary layer is given as follows:

$$\frac{\partial u}{\partial t} + u \frac{\partial u}{\partial x} + w \frac{\partial u}{\partial z} = -\frac{1}{\rho_f} \frac{\partial p}{\partial x} + \frac{1}{\rho_f} \frac{\partial \tau}{\partial z} \tag{1}$$

in which t is the time, p is the pressure, ρ_f is the density of fluid, and τ is the shear stress. If the mean flow is parallel to the

bed, Eq.(1) is reduced to

$$\frac{\partial u}{\partial t} = -\frac{1}{\rho_f} \frac{\partial p}{\partial x} + \frac{1}{\rho_f} \frac{\partial \tau}{\partial z} \quad (2)$$

The pressure gradient just outside the boundary layer is given by

$$-\frac{1}{\rho_f} \frac{\partial p}{\partial x} = \frac{\partial u_b}{\partial t} \quad (3)$$

in which u_b is the horizontal velocity at the upper edge of the boundary layer.

If the above expression also holds in the boundary layer, Eq.(2) becomes

$$\frac{\partial(u - u_b)}{\partial t} = \frac{1}{\rho_f} \frac{\partial \tau}{\partial z} \quad (4)$$

(b) Concentration

The one-dimensional turbulent diffusion equation for sediment concentration is given as follows:

$$\frac{\partial C}{\partial t} + w \frac{\partial C}{\partial z} = \frac{\partial}{\partial z} \left(K_z \frac{\partial C}{\partial z} \right) + w_0 \frac{\partial C}{\partial z} \quad (5)$$

in which C is the sediment concentration, K_z is the turbulent diffusion coefficient, and w_0 is the settling velocity of sediment.

4.2 Initial and boundary conditions

Eqs.(4) and (5) were solved numerically using a finite difference method with Crank-Nicholson implicit scheme. The initial and boundary conditions for Eq.(4) are

$$\begin{aligned} u(z, 0) &= 0 \\ u(z_0, t) &= 0 \\ u(\delta_b, t) &= u_b(t) \end{aligned} \quad (6)$$

in which z_0 is the roughness length and δ_b is the thickness of the turbulent boundary layer. Initial and boundary conditions for Eq.(5) are

$$\begin{aligned} C(z, 0) &= 0 \\ C(\delta_B, t) &= C_0(t) \\ K_z \frac{\partial C}{\partial z} + w_0 C &= 0, \quad z = h \end{aligned} \quad (7)$$

in which δ_B is the thickness of the bed-layer, $C_0(t)$ is the sediment concentration in the bed-layer, and h is the water depth.

4.3 Evaluations of parameters

The vertical distance from the bottom to the water surface is divided by 101 points. The vertical distance from the bottom to the level of three grain diameters is divided into the interval of one-half a grain diameter, and above the level the intervals are determined so as to form a geometric progression. The computational time-step is

determined as $T / 96$ (T : the wave period).

(a) Velocity in the boundary layer

The eddy viscosities are assumed to be

$$Nz(z) = \alpha \kappa \sqrt{f} u_{bm} z \quad (8-1)$$

$$Nz(z, t) = \alpha \kappa \sqrt{f} |u_b(t)| z \quad (8-2)$$

where α is the constant of proportionality, κ is the Karman constant, f is the bottom friction factor and u_b is the maximum velocity at the upper edge of the boundary layer. Bottom friction factor is calculated from the empirical expression given by Kakinuma and Ifuku(1985):

$$\begin{aligned} f &= 1.95\theta^{-0.87} & 2 \leq \theta \leq 40 \\ f &= 0.39\theta^{-0.42} & 40 \leq \theta \leq 190 \end{aligned} \quad (9)$$

where $\theta = \rho_f u_{bm}^3 / (\rho_s - \rho_f) g d_{50}$, ρ_s is the density of sediment ($\rho_s = n\rho_f + (1-n)\rho_s'$, n is the porosity, ρ_s' is the density of dry sediment), g is the acceleration gravity, and d_{50} is the median diameter of sediment.

The roughness length, according to Bakker-van Doorn(1978), is

$$z_0 = \eta / 33 \quad (10)$$

where η is the ripple height, which is estimated from Nielsen's empirical relationship(1981):

$$\eta = 21 a_m \theta^{-1.85} \quad (11)$$

where a_m is the half stroke of water particle at the bottom.

Noda(1969) evaluated the thickness of turbulent boundary layer as

$$\delta_b = 25\delta \quad (12)$$

where $\delta = \sqrt{\nu T / 2\pi}$ (ν : the kinematic viscosity). At each point, until the difference of normalized velocity between the times of mT (m : integer) and $(m+1)T$ becomes less than 10^{-5} , calculation is continued.

(b) Concentration

The sediment concentration in the bed-layer, according to Kalkanis(1965), is

$$C_0 = 2P\rho_s d \cdot V / 3 \int_{z_0}^{\delta_b} u dz \quad (13)$$

where d is the particle size of sediment, V is the speed of sediment propagation and P is the pick-up rate:

$$P = \frac{1}{\sqrt{2\pi}} \int_{B_* \Psi^{-1} / \eta_0}^{\infty} \exp(-z^2/2) dz \quad (14)$$

where $B_* = 4/3 C_L \eta_0$, C_L is the lift coefficient, $1/\eta_0$ is an empirical constant, and $\Psi' = (\rho_s - \rho_f) g d / \rho_f u_0^2$ (u_0 : the local water particle velocity). It is difficult to estimate the speed of sediment propagation in Eq.(13). In the present analysis it is set to be equal to the cross-sectional mean velocity of water particles in the bed-layer.

The turbulent diffusion coefficients are assumed to be

$$K_z = \beta \alpha \sqrt{\bar{f}} u_{bm} z \quad (15-1)$$

$$K_z = \beta \alpha \sqrt{\bar{f}} |u_b(t)| z \quad (15-2)$$

$$K_z = \gamma (l_T u^2 + l_L w^2) / q \quad (15-3)$$

where β, γ are the constant of proportionality, l_T and l_L are the characteristic length ($l_L = \alpha l_T$; α : the constant of proportionality), and $q = (u^2 + w^2)^{1/2}$.

The settling velocity of sediment is calculated by

$$w_0 = \sqrt{\frac{4}{3} \frac{d}{C_D} \frac{\rho_s - \rho_f}{\rho_f} g} \quad (16)$$

where C_D is the drag coefficient. In the case of Reynolds number, $Re = w_0 d / \nu$ being less than 5, the drag coefficient can be estimated (1968) by

$$C_D = \frac{24}{Re} + 4.5 \quad (17)$$

At each point until the difference of normalized concentration between the times of mT and $(m+1)T$ is less than 10^{-5} , calculation is continued. In the present study, the fluids are sea water for Noda's, the authors' and Nielsen's observed results and fresh water for the results obtained by Deigaard et al. The water temperatures are assumed to be 10°C for the authors' results and 20°C for the others' results. The sediment is sand and density and porosity have been taken at 2.65 g/cm^3 and 0.3 respectively. Sand grain sizes are $0.30, 0.18, 0.12-0.22$ and 0.12 mm for Noda's, the authors', Nielsen's and Deigaard et al. results, respectively. The characteristic length, l_T , is assumed to be the distance from the bottom.

5. Numerical results

Parametric analysis is performed by using the observed data obtained by Noda, the authors and Nielsen and measured data by Deigaard et al. The significant waves obtained through field observations by Nada, authors and Nielsen and laboratory measurement by Deigaard et al., are in the range that Stokes wave theory of second order, third order and cnoidal wave theory and Stokes wave third order are valid (1977), respectively. Einstein and El-Samni (1949) reported that the lift coefficient has a constant value 0.178 on the basis of measurement of the pressure difference. It was assumed here that the lift coefficient is 0.2 and $1/\eta$ is 1.5 after Kalkanis and w_0 has been taken to be the value at the top of the sand particle and the thickness of the bed-layer is twice sand particle.

5.1 Velocity in the turbulent boundary layer

The velocity profiles at various phases during a cycle of wave motion in the turbulent boundary layer are shown in Fig. 5. The maximum value of the water particle velocity at phase 6 is approximately 1.03 times as

large as that at the upper edge of boundary layer. In the case that the shear stress is evaluated by using time-dependent eddy viscosity or Prandtl mixing length theory the over-shooting is more significant than the case that the shear stress is evaluated by using time-independent eddy viscosity at phases 6.25, 6.375, 6.5 and 6.875 and the levels which arise the over-shooting are lower at above-mentioned phases where the water particle velocities are negative. In the cases that the shear stress is evaluated by using time-dependent eddy viscosity and Prandtl mixing length theory, both profiles show the similar trend.

Fig.6 shows the temporal variation of water particle velocity at the sand particle level. The velocity profiles are asymmetric and the phase of the maximum velocity is ahead of that at the upper edge of boundary layer by approximately $\pi/12$.

5.2 Concentration

(a) Variation of sediment concentration in the bed-layer

Fig.7 shows the variation of the sediment concentration in the bed-layer depending on the instantaneous value of $1/\psi'$. The concentration in the bed-layer is calculated on the assumption that the thickness of the bed-layer is equal to twice the grain diameter in Eq.(13). For larger value of $1/\psi'$ in the range of present analysis, the concentration in the bed-layer is asymptotic to about 0.3. This tendency is similar to the result obtained by Deigaard et al.(1986).

(b) Temporal variation of sediment concentration at several heights

Fig.8 shows the temporal variation of suspended sediment concentration; in (a)-(f) are in the cases that the relative heights are 1.67×10^{-4} , 1.44×10^{-3} , 2.44×10^{-3} , 1.22×10^{-2} , 1.93×10^{-2} and 2.41×10^{-2} respectively. With being off from the bottom, suspended sediment concentration decreases and the peak of suspended sediment concentration leads gradually. At $z/h=1.93 \times 10^{-2}$, is the height at which suspended sediment concentrations are observed, the peak of suspended sediment concentration appears at phase 6.25 approximately. It is the phase where the cross-shore velocity at the upper edge reverses approximately.

(c) Temporal variation of sediment concentration and phase lag between cross-shore velocity and sediment concentration

Fig.9 shows the computed temporal variations of suspended sediment concentration at 0.04 m from the bottom in comparison with the histogram of phase lag between maximum value of observed onshore velocity and maximum value of suspended sediment concentration during a wave cycle. Peaks in the histogram are found at $\pi/2$ and 1.3π in (a) and $\pi/2$ and 1.1π in (b)-corresponding to peaks in the computed temporal variation of suspended sediment concentration. The temporal variation, calculated by using time-independent turbulent diffusion coefficient, has its peaks at the above-mentioned phases; but the value of both peaks is approximately the same, and the computed temporal variation disagrees with the histogram of phase lag. The temporal variations which are computed by using time-dependent turbulent diffusion coefficient has its peaks at the above-mentioned phases and the agreement between that computed and observed is good. It is, however, worth noting that the computed temporal variation which is computed by using Eq.(15-3) could

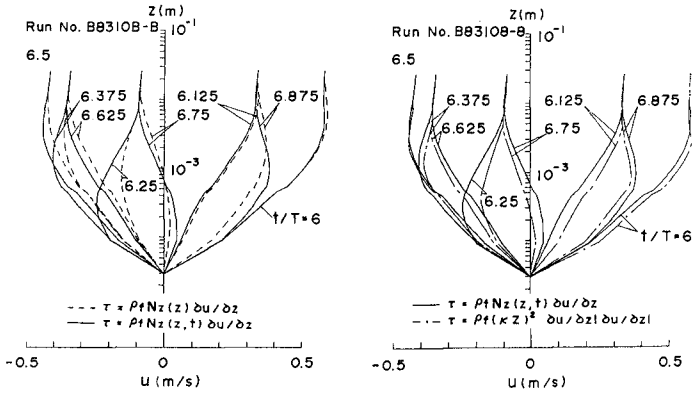


Fig.5 Velocity distributions in the turbulent boundary layer.

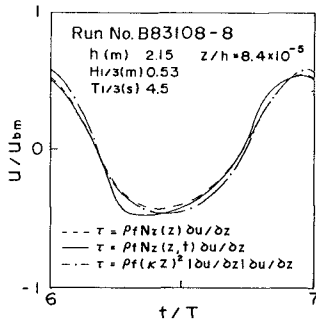


Fig.6 Temporal variations of water particle velocity at the sand particle level.

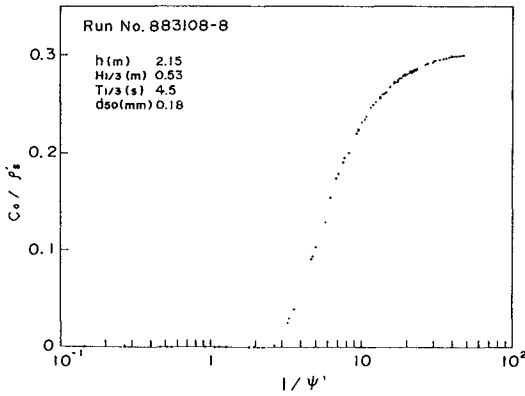


Fig.7 Relationship between the concentration in the bed-layer and $1/\psi'$.

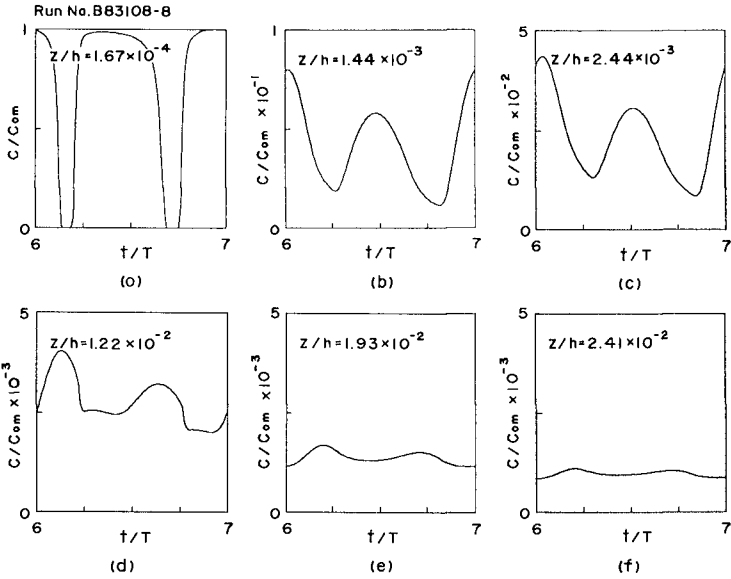


Fig.8 Temporal variations of suspended sediment concentration.

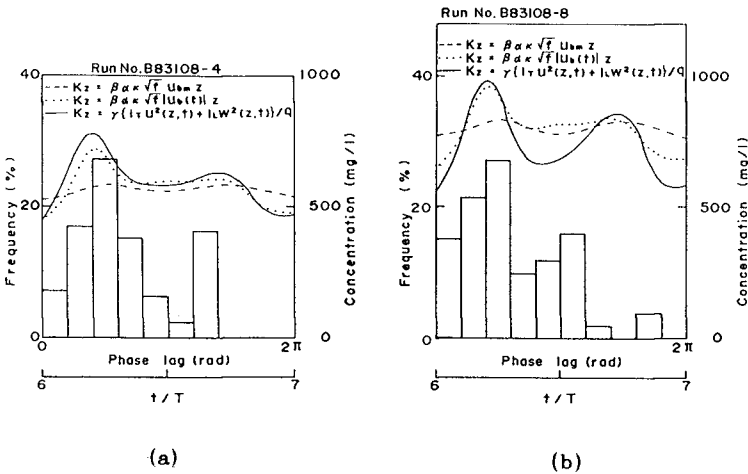


Fig.9 Computed temporal variations of suspended sediment and histogram of phase lag between maximum onshore velocity and maximum concentration observed in a wave cycle, where the frequencies of breaker occurrence are (a) 13% and (b) 19%.

elucidate the histogram of phase lag better than one computed by using Eq.(15-2).

(d) Vertical distributions of sediment concentration

Fig.10 shows the distributions of the computed suspended sediment concentration averaged over a wave cycle in comparison with those observed. The broken, solid and dotted lines are in the case that the shear stresses are evaluated by using Eq.(8-2) and the turbulent diffusion coefficients are evaluated by using Eqs.(15-1),(15-2) and (15-3) respectively. In the present analysis the constant of proportionality, α , in Eq.(8-2) is set to be equal to 0.1. The steepening of the profiles occurs at lower level above the bottom. However, the computed distributions that the turbulent diffusion coefficients are evaluated by using Eqs.(15-1) and (15-2) could not elucidate the suspended sediment concentration at higher levels above the bottom. It is,however,worth noting that the distribution of suspended sediment concentration calculated by using Eq.(15-3) could elucidate the concentration at the level farther from the bottom.

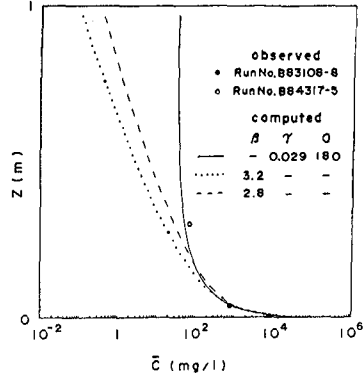


Fig.10 Distributions of mean suspended sediment concentration.

Fig.11 shows the distributions of the computed mean suspended sediment concentration in comparison with those observed; (a) and (b) are in the case of non-breaking wave by Noda and plunging breaker by Nielsen. The solid and dot-dash lines are in the case that the shear stresses are evaluated by using time-dependent eddy viscosity and Eq.(8-2) and the turbulent diffusion coefficient is evaluated by using Eq.(15-3) respectively. In the present analysis the constant of proportionality, α , in Eq.(8-2) is set to be equal to 0.1. Though exhibiting appreciable discrepancy, the computed distributions agree well with those observed.

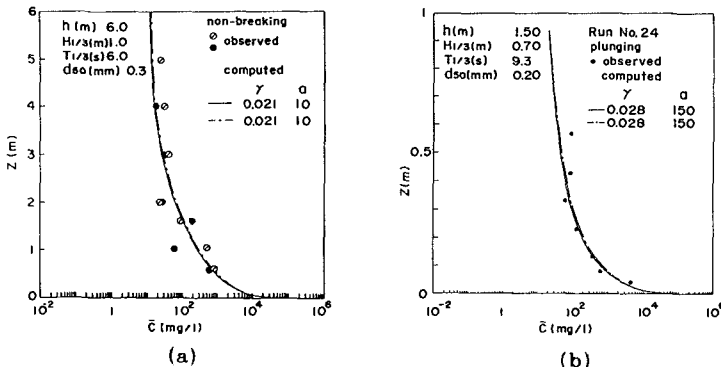


Fig.11 Distributions of mean suspended sediment concentration; (a) Noda's data, (b) Nielsen's data.

5.3 Relationship between γ , a and characteristics of wave and bed material

Fig.12 shows the relationship between the constant of proportionality γ in Eq.(15-3) and the ratio of significant wave height to the median diameter $H_{1/3}/d_{50}$. With increasing $H_{1/3}/d_{50}$, the constant of proportionality, γ , decreases. For the same value of $H_{1/3}/d_{50}$, the constant of proportionality, γ , is largest for the plunging breaker.

Fig.13 shows the relation between the constant of proportionality, a , in Eq.(15-3) and the ratio of significant wave height to the mean water depth, the constant of proportionality, a , increases.

5.3 Turbulent diffusion coefficient

Fig.14 shows the distributions of the nondimensional turbulent diffusion coefficient which could elucidate the observed distributions of suspended sediment concentration; (a) and (b) are in the case of non-breaking wave by Noda and plunging breaker by Nielsen respectively. In this figure solid lines represent the instantaneous values of turbulent diffusion coefficient and the broken line represents the value averaged over a wave cycle. The symbols represent the value computed by Eq.(18) on the basis of the distributions of mean suspended sediment concentration. The nondimensional turbulent diffusion coefficient averaged over a wave cycle is proportional to z/h from the bottom to the level that the relative height is approximately 0.1 and proportional to $(z/h)^2$ at levels farther from the bottom.

$$\bar{K}_z = -w_0 \bar{C} / (\partial \bar{C} / \partial z) \quad (18)$$

where \bar{C} is the time-averaged sediment concentration.

6. Conclusions

Velocity, pressure fluctuation and suspended sediment concentration were measured near the bottom in the surf zone. The results were discussed in comparison with the calculated velocity distribution in the turbulent boundary layer and suspended sediment concentration. The following conclusions have been obtained through the present study.

(1) The histogram of phase lag between maximum concentration and maximum onshore velocity during a wave cycle exhibit peaks at phases $\pi/2$ and 1.1π or 1.3π .

(2) Good agreement between the observed results and the computed results is obtained concerning the phase lag between concentration and water particle velocity and mean value of suspended sediment concentration.

(3) The turbulent diffusion coefficient averaged over a wave cycle is proportional to z/h near the bottom and proportional to $(z/h)^2$ near the water surface.

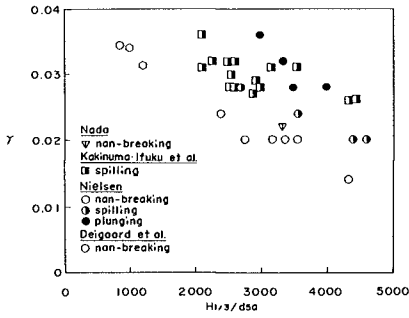


Fig.12 Proportional constant, γ as a function of $H_{1/3}/d_{50}$.

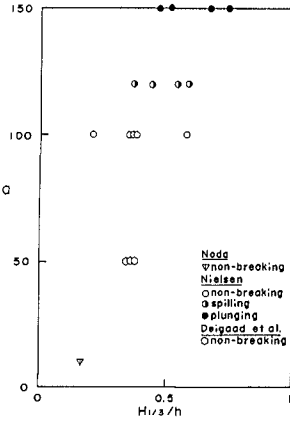


Fig.13 Proportional constant, α as a function of $H_{1/3}/h$.

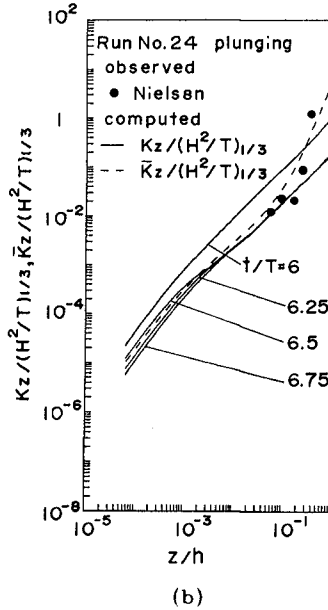
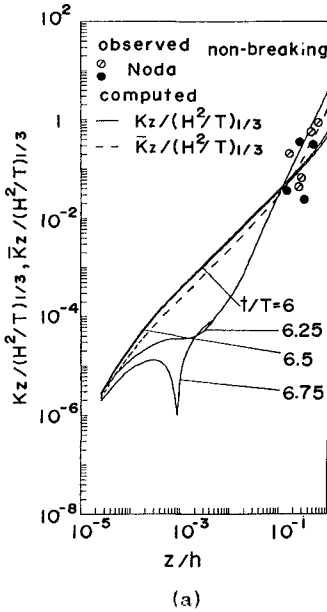


Fig.14 Nondimensional turbulent diffusion coefficient as a function of relative height.

References

- 1) Bakker, W.T. and Th. van Doorn(1978): Near bottom velocities in waves with a current, Proc. 16th Coastal Eng. Conf., pp.1394-1413.
- 2) Brenninkmeyer, B.M.(1974): Mode and period of sand transport in the surf zone, Proc. 14th Coastal Eng. Conf., pp.812-827.
- 3) Deigaard, R., J.Fredsoe and I.B. Hedegaard(1986): Suspended sediment in the surf zone, J. Waterway, Port, Coastal and Ocean Eng., ASCE, pp.115-128.
- 4) Einstein, H.A. and El-Samni El. S.A.(1949): Hydrodynamic forces on a rough wall, Rev. Mod. Phys., pp.520-524.
- 5) Fairchild, J.C.(1959): Suspended sediment sampling in oscillatory wave action, Beach Erosion Board, Tech. Memo 115p..
- 6) Homma, M. and K. Horikawa(1962): Suspended sediment due to wave action, Proc. 8th Coastal Eng. Conf., pp.168-193.
- 7) Homma, M., K. Horikawa and R. Kajima(1965): A study on suspended sediment due to wave action, Coastal Eng. Japan, Vol.8, pp.85-103.
- 8) Kakinuma, T. and M. Ifuku(1985): Bottom friction factor on beaches, Proc. 32nd Japanese Conf. Coastal Eng., pp.234-237.(in Japanese)
- 9) Kalkanis, G.(1965): Transportation of bed material due to wave action, U.S.Army, Coastal Res.Center, Tech. Memo 2, pp.1-114.
- 10) Kestin, J.(1968): Boundary Layer Theory, 6th ed. McGraw Hill, p.108.
- 11) Nielsen, P.(1981): Dynamics and geometry of wave generated ripples, J.G.R., Vol.86, No.C7, pp.6467-6472.
- 12) Noda, H.(1967): Sediment suspension by waves, Proc. 14th Japanese Conf. Coastal Eng., pp.306-314.(in Japanese)
- 13) Noda, H.(1969): Development of turbulent boundary layer by waves, Proc. 16th Japanese Conf. Coastal Eng., pp.23-27.(in Japanese)
- 14) Sleath, J.F.A.(1982): The suspension of sand by waves, J. Hydraul. Res., Vol.19, pp.439-452.
- 15) U.S.Army Coastal Eng. Res. Center(1977): Shore Protection Manual, Vol.2, p.35.
- 16) Wright, L.D., R.T.Guza and A.D. Short(1982): Dynamics of high energy dissipative surf zone, Marine Geology, Vol.45, pp.41-61.